Received: 5 December 2024 | Revised: 24 March 2025 | Accepted: 29 March 2025

DOI: 10.1002/alz.70242

RESEARCH ARTICLE

Alzheimer's & Dementia®
THE JOURNAL OF THE ALZHEIMER'S ASSOCIATION

Relationships between neuropsychiatric symptoms, subtypes of astrocyte activities, and brain pathologies in Alzheimer's disease and Parkinson's disease

Oceanna Yueran Li | **Steven Shin** | **Sa Zhou** | **Adam Turnbull** | **F. Vankee Lin** | **for the Alzheimer's Disease Neuroimaging Initiative**

CogT Lab, Department of Psychiatry and Behavioral Sciences, Stanford University, Stanford, California, USA

Correspondence
F. Vankee Lin, 1070 Arastradero Road, CA 94304, USA.
Email: vankee_lin@stanford.edu

Data used in preparation of this article were obtained from the Alzheimer's Disease Neuroimaging Initiative (ADNI) database (adni.loni.usc.edu). As such, the investigators within the ADNI contributed to the design and implementation of ADNI and/or provided data but did not participate in analysis or writing of this report. A complete listing of ADNI investigators can be found at: http://adni.loni.usc.edu/wp-content/uploads/how_to_apply/ADNI_Acknowledgement_List.pdf

Abstract

INTRODUCTION: Alzheimer's disease (AD) and Parkinson's disease (PD) are neurodegenerative diseases (NDs). This study examined astrocytic contributions to neuropsychiatric symptoms (NPS), focusing on astrocytic protein activity and its relationship with NPS severity, accounting for clinical and pathological features of NDs.

METHODS: Cerebrospinal astrocytic proteins (glial fibrillary acidic protein [GFAP], chitinase-3-like protein 1 [YKL-40], and aquaporin-4 [AQP4]) from Alzheimer's Disease Neuroimaging Initiative (ADNI) (AD) and Parkinson's Progression Markers Initiative (PPMI) (PD) were analyzed using K-means clustering. Six NPS domains, ND-specific pathologies (amyloid-beta/Aβ for AD, alpha-synuclein/αSyn for PD), and nonspecific pathology (phosphorylated tau/ptau) were assessed.

RESULTS: In both samples, three astrocytic clusters were identified, and the "highYKL|lowOthers" cluster (high YKL-40, low GFAP/AQP4) consistently showed lower ptau and NPS severity compared to the "highAll" cluster (high GFAP, YKL-40, AQP4). In PPMI, the "highYKL|lowOthers" cluster also attenuated the relationship between αSyn and NPS compared to the "highAll" cluster.

Oceanna Yueran Li and Steven Shin contributed equally to this work.

Funding information: Alzheimer's Disease Neuroimaging Initiative; National Institutes of Health, Grant/Award Numbers: U01 AG024904, U24AG072701, 1K01AG086665; DOD ADNI, Grant/Award Number: W81XWH-12-2-0012; ADNI; National Institute on Aging; National Institute of Biomedical Imaging and Bioengineering; AbbVie; Alzheimer's Association; Araclon Biotech; Biogen; CereSpir, Inc.; Cogstate; Eisai Inc.; Elan Pharmaceuticals, Inc.; Eli Lilly and Company; Euroimmun; Genentech, Inc.; Fujirebio; GE Healthcare; IXICO Ltd.; Janssen Alzheimer Immunotherapy Research & Development, LLC.; Johnson & Johnson Pharmaceutical Research & Development LLC.; Lumosity; Lundbeck; Meso Scale Diagnostics, LLC.; NeuroRx Research; Neurotrack Technologies; Novartis Pharmaceuticals Corporation; Pfizer Inc.; Piramal Imaging; Takeda Pharmaceutical Company; Transition Therapeutics; Canadian Institutes of Health Research; Northern California Institute for Research and Education; Alzheimer's Therapeutic Research Institute; University of Southern California; Laboratory for Neuro Imaging at the University of Southern California; Michael J. Fox Foundation for Parkinson's Research; 4D Pharma; Abbvie; AcureX; Allergan; Amathus Therapeutics; Aligning Science Across Parkinson's; AskBio; Avid Radiopharmaceuticals; BIAL; BioArctic; Biohaven; BioLegend; BlueRock Therapeutics; Calico Labs; Capsida Biotherapeutics; Celgene; Cerevel Therapeutics; Coave Therapeutics; DaCapo Brainscience; Denali; Edmond J. Safra Foundation; Eli Lilly; Gain Therapeutics; Genentech; GSK; Golub Capital; Handl Therapeutics; Insitro; Jazz Pharmaceuticals; Johnson & Johnson Innovative Medicine; Merck; Meso Scale Discovery; Mission Therapeutics; Neurocrine Biosciences; Neuron23; Neuropore; Pfizer; Piramal; Prevail Therapeutics; Roche; Sanofi; Servier; Sun Pharma Advanced Research Company; Takeda; Teva; UCB; Vanqua Bio; Verily; Voyager Therapeutics; Weston Family Foundation; Yumanity Therapeutic

DISCUSSION: Astrocytic activity relates to NPS, highlighting astrocytic proteins as potential therapeutic targets for NPS in NDs.

KEYWORDS
Alzheimer's disease, astrocyte, neuropsychiatric symptoms, Parkinson's disease, tauopathy

Highlights

- Astrocytic protein clusters were linked to NPS severity in AD and PD cohorts.
- The "highYKL|lowOthers" cluster showed lower ptau and NPS severity than "allhigh" cluster in AD and PD cohorts.
- Astrocytic proteins may serve as therapeutic targets for managing NPS in NDs.

1 | BACKGROUND

Neurodegenerative diseases (NDs) are primarily characterized by cognitive decline and movement impairment.[1] However, researchers are increasingly recognizing neuropsychiatric symptoms (NPS) as a significant aspect of these diseases. In Alzheimer's disease (AD) and Parkinson's disease (PD), two of the most prevalent NDs, NPS such as depression, anxiety, apathy, agitation, irritability, sleep disturbances, disinhibition, and hallucinations are frequently observed and are increasingly being integrated into the diagnosis of dementia or prognosis of dementia progression.[1–3] However, our current understanding of the neurobiological mechanisms underlying NPS is limited, often focusing primarily on neuronal dysfunctions.[4] Emerging evidence suggests that non-neuronal cells play an often-overlooked role in regulating neuronal function[5] and complex behaviors like NPS.[6] For example, optogenetic activation of astrocytes can trigger the low-frequency state of a cortical circuit and alter sleep patterns.[7] Also, studies in mouse models exhibiting NPS suggest that astrocytes are central to NPS through various mechanisms, including altered Ca2+ signaling, disrupted gliotransmission, and dysregulated ionic and metabolic homeostasis, hormone signaling, and inflammation.[6,8–11] Integrating astrocytes into the study of NPS could provide insights into non-neuronal contributions to NPS, with the potential of uncovering novel therapeutic strategies.

Human studies examining astrocytes and NPS are still in their infancy. Emerging studies have examined astrocytic gene expression, revealing region-specific differences in human astrocytes,[6] and *post-mortem* analyses have highlighted decreased astrocyte density[12] and increased astrocyte dysfunction[13] in selected brain regions associated with psychiatric disorders. When conducting in vivo studies in older adults with NDs, astrocytes show considerable variation in their responses to aging and ND pathologies, and are heterogeneous in older adults, including those with different types of NDs.[14,15] Further, differing insults and inflammatory conditions can induce distinct astrocyte activity that is either neuroprotective or neurotoxic.[16,17] Cerebrospinal fluid (CSF) based measures of astrocyte activity, most widely studied in glial fibrillary acidic protein (GFAP),[18–20] chitinase-3-like protein 1 (YKL-40),[19,21,22] and aquaporin-4 (AQP4)[23–25] all have complex, and often inconsistent relationships with ND pathologies and dementia stages, as well as between these astrocyte biomarkers themselves,[19,21,26,27] across studies.

Given the complicated and likely non-linear relationships between astrocytic activity and the varied pathological and clinical presentation of NDs, as well as the diverse response phenotypes of astrocytes to pathophysiology,[28] traditional approaches, which look for direct linear relationships between ND symptoms and individual biomarkers, may fail to account for the extensive heterogeneity of astrocytic activity in various environments. For this reason, the present study characterizes astrocytic protein levels according to three biomarkers with unique functions and/or responses to brain aging – GFAP, AQP4, and YKL-40 – using a clustering-based analysis. We question whether distinct subtypes of astrocytic activity can be used to explain differences in the presentation of NPS within AD and PD. By clustering samples based on multiple astrocytic proteins, we can better understand the ways in which astrocytes relate to ND progression in distinct neuropathological contexts. Similar approaches, using data-driven clustering of neuroimaging or biomarker data, have been successfully applied to uncover important pathological subtypes and their associations with specific functional outcomes.[29] Accordingly, we tested the following hypotheses: (1) We anticipate discovering both similar and distinct clusters of astrocytic biomarkers between NDs; the differences in astrocyte patterns between NDs are expected to be associated with disease-primary pathologies (amyloid-beta/Aβ for AD and α-synuclein/αSyn for PD) and similarities are expected to be associated with pathology that is generic to biological aging (such as phosphorylated tau/ptau); (2) We expect to find shared associations between selected astrocyte clusters and the severity of NPS across NDs, independent of the clinical or pathological severity of ND.

The study utilized the Alzheimer's Disease Neuroimaging Initiative (ADNI) and the Parkinson's Progression Markers Initiative (PPMI) datasets. In addition to requiring CSF-based astrocytic protein markers, we focused on patients with preclinical and clinical NDs (i.e., mild cognitive impairment [MCI] and AD dementia in ADNI, and prodromal PD and PD in PPMI) given our interest in the presence or absence of NPS in preclinical and clinical NDs. The process for sample selection

across the two datasets is detailed in Figure 1, and the main variables across the two datasets are detailed in Table 1.

2 | METHODS

2.1 | Data source

2.1.1 | ADNI

Data used in the preparation of this article were obtained from the ADNI database (adni.loni.usc.edu). The ADNI was launched in 2003 as a public-private partnership, led by Principal Investigator Michael W. Weiner, MD. The primary goal of ADNI has been to test whether serial magnetic resonance imaging (MRI), positron emission tomography (PET), other biological markers, and clinical and neuropsychological assessment can be combined to measure the progression of MCI and early AD.

2.1.2 | PPMI

PPMI is a global observational study aimed at creating biomarker-defined groups and identifying clinical, imaging, genetic, and biospecimen markers to track the progression of PD. This effort seeks to accelerate the development of disease-modifying therapies. The PPMI steering committee oversees all aspects of the study, coordinating its operations across clinical, imaging, genetic, bioanalytical, biorepository, statistical, and bioinformatics cores. The committee comprises experts in PD clinical research and biomarkers, core leaders, representatives from the Michael J. Fox Foundation for Parkinson's Research, and scientists from the industry.[30]

2.2 | Participants

2.2.1 | ADNI

Participants in this study were from ADNI GO and ADNI2. For primary analysis, we selected participants based on (1) availability of CSF proteomics (Aβ, ptau, αSyn, YKL-40, GFAP, AQP4) data at baseline, (2) availability of the Neuropsychiatric Inventory (NPI) measuring NPS, and (3) having MCI or AD diagnoses. Our sample is limited to the ADNI GO/2 cohort because SOMAscan CSF-based proteomics data were only available in select samples with stable diagnosis in ADNI GO/2. The final sample contained 289 participants with their background characteristics provided in Table 2.

2.2.2 | PPMI

For primary analyses, we selected participants based on (1) availability of CSF proteomics (Aβ, ptau, αSyn, YKL-40, GFAP, AQP4) data at baseline; (2) availability of the following measurements for NPS: Movement Disorder Society-Unified Parkinson's Disease Rating Scale (MDS-UPDRS) 1.2 Hallucinations and Psychosis, MDS-UPDRS 1.5 Apathy, MDS-UPDRS 1.7 Sleep Problems, MDS-UPDRS 1.8 Daytime Sleepiness, State-Trait Anxiety Inventory (STAI), Geriatric Depression Scale (GDS), and Questionnaire for Impulsive-Compulsive Disorders in Parkinson's Disease (QUIP); (3) having prodromal PD or PD diagnoses; and (4) age $\geq$ 65 to match the mean age of the included ADNI sample since the age range in PPMI was wide. The final sample contained 378 participants with their background characteristics provided in Table 2.

RESEARCH IN CONTEXT

1. **Systematic review**: This study examines the role of astrocytic activity in neuropsychiatric symptoms (NPS) in Alzheimer's disease (AD) and Parkinson's disease (PD), focusing on cerebrospinal fluid astrocyte related biomarkers—glial fibrillary acidic protein (GFAP), chitinase-3-like protein 1 (YKL-40), and aquaporin-4 (AQP4). While astrocytes have been increasingly recognized as key players in these diseases, prior research has primarily emphasized neuronal mechanisms. Leveraging data from two large cohorts, Alzheimer's Disease Neuroimaging Initiative (ADNI) and Parkinson's Progression Markers Initiative (PPMI), this study explores how astrocytic activity influences the severity of NPS in both AD and PD.
2. **Interpretation**: Shared astrocytic patterns were identified across AD and PD cohorts, with clusters distinguished by varying levels of GFAP and AQP4. These clusters correspond to differences in pathology levels (ptau, Aβ, αSyn) and NPS severity. Clusters characterized by lower GFAP and AQP4 levels were associated with lower pathology burden and NPS severity, and a weaker relationship between pathology and NPS, suggesting a potentially protective astrocytic response.
3. **Future directions**: This study highlights the need for further research into how astrocyte function, particularly in response to specific neurodegenerative pathologies, affects NPS. Longitudinal studies and advanced biomarker analyses are essential to deepen our understanding of astrocytes' roles in neurodegenerative disease progression and to identify therapeutic targets for managing NPS in AD and PD.

2.3 | Measures

2.3.1 | Neuropsychiatric symptoms measure

ADNI

NPS were measured via NPI,[31] based on informant report regarding symptoms in the past 4 weeks. For each subdomain, we multiplied

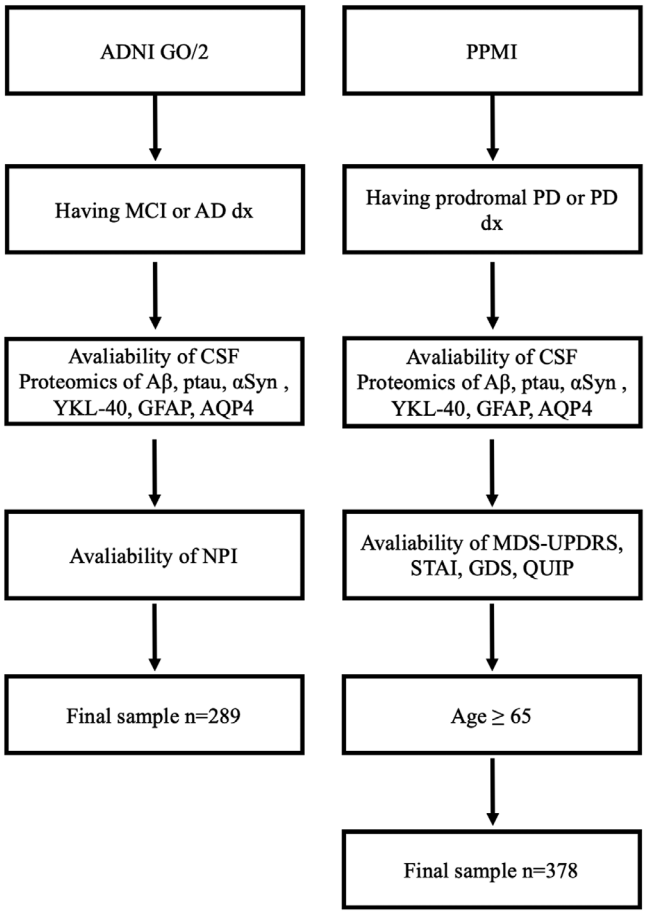

FIGURE 1 Sample selection flowchart across ADNI and PPMI. ADNI, Alzheimer's Disease Neuroimaging Initiative; Aβ, amyloid-beta; AQP4, aquaporin-4; αSyn, alpha-synuclein; AD, Alzheimer's disease; CSF, cerebrospinal fluid; Dx, diagnosis; GDS, Geriatric Depression Scale; GFAP, glial fibrillary acidic protein; MCI, mild cognitive impairment; MDS-UPDRS, Movement Disorder Society Unified Parkinson's Disease Rating Scale; NPI, Neuropsychiatric Inventory; PD, Parkinson's disease; PPMI, Parkinson's Progression Markers Initiative; ptau, phosphorylated tau; QUIP, Questionnaire for Impulsive-Compulsive Disorders in Parkinson's Disease; STAI, State-Trait Anxiety Inventory; YKL-40, chitinase-3-like protein 1.

TABLE 1 Main variables across two ADNI and PPMI datasets.

Parameter	ADNI GO/2	PPMI
CSF Aβ	☑	☑
CSF ptau	☑	☑
CSF αSyn	☑	☑
CSF GFAP	☑	☑
CSF YKL-40	☑	☑
CSF AQP4	☑	☑
Measure in Delusions	☑	
Measure in Hallucinations	☑	☑
Measure in Agitation/Aggression	☑	
Measure in Depression/Dysphoria	☑	☑
Measure in Anxiety	☑	☑
Measure in Elation/Euphoria	☑	
Measure in Apathy/Indifference	☑	☑
Measure in Disinhibition/Compulsive Behavior	☑	☑
Measure in Irritability/Lability	☑	
Measure in Motor Disturbance	☑	
Measure in Sleep and Nighttime Behaviors	☑	☑
Measure in Appetite/Eating	☑	

Abbreviations: αSyn, alpha-synuclein; Aβ, amyloid-beta; ADNI, Alzheimer's Disease Neuroimaging Initiative; AQP4, aquaporin-4; CSF, cerebrospinal fluid; GFAP, glial fibrillary acidic protein; PPMI, Parkinson's Progression Markers Initiative; ptau, phosphorylated tau; YKL-40, chitinase-3-like protein 1.

the frequency by its severity. Since our primary aim was to examine the similarities and differences in the relationships between astrocytic activity and NPS between distinct NDs, we primarily focused on the subdomains of NPS that are comparable between ADNI and PPMI, and used the sum of six subdomain scores across apathy/indifference, hallucinations, sleep and nighttime behaviors, depression/dysphoria, anxiety, and disinhibition/compulsive behavior as the primary measure of NPS. We also calculated the traditional total sum across all 12 subdomains as the secondary measure. Z-scores were used for both individual subdomain scores and total scores.

PPMI

NPS were measured using MDS-UPDRS Hallucinations and Psychosis for hallucinations, Apathy for apathy/indifference, Sleep Problems and Daytime Sleepiness for sleep and nighttime behaviors via a combination of participant's self-report with or without caregiver's assistance, and investigator's assessment, focusing on symptoms experienced over the past 1 week.[32,33] Anxiety was measured using the STAI, where participants reported their current feelings for state anxiety and their general feelings for trait anxiety, with a total score used combining state and trait anxiety.[34] Depression/dysphoria was evaluated using GDS, with participants self-reporting for the past 1 week.[35] Disinhibition/compulsive behaviors were assessed using QUIP, which captured self-reported behaviors lasting more than 4 weeks.[36] A composite score of the six domains, calculated as the mean of the z-score transformed values for each domain, were used in the main analysis and z-scores for the six individual subdomains were used in the post-hoc analysis.

2.3.2 | CSF biomarkers

ADNI

The lumbar puncture procedure in ADNI is described in the ADNI procedure manual (https://adni.loni.usc.edu/wp-content/uploads/2010/09/CSF_Sample_Proposal_yr2-3.pdf). CSF GFAP, YKL-40, AQP4, and

TABLE 2 ADNI and PPMI sample characteristics.

Parameter	ADNI sample ($n = 289$)	PPMI sample ($n = 378$)
Years of age, Mean+/-SD	72.64+/- 8.03	70.34+/- 4.13
Men, *N* (%)	163 (58.0%)	216 (57.1%)
Education (years), Mean +/-SD	16.16+/- 2.70	16.06+/- 3.78
MCI (in ADNI) or prodromal PD (in PPMI), *N* (%)	213 (73.7%)	263 (69.6%)
CSF-based GFAP^, Mean +/-SD	3.61+/- 0.20	2.51+/- 0.04†
CSF-based YKL-40^, Mean +/-SD	11.83+/- 0.45	2.80+/- 0.04†
CSF-based AQP4^, Mean +/-SD	5.12+/- 0.03	1.89+/- 0.04†
CSF-based Aβ^, Mean +/-SD	6.70+/- 0.50	6.71+/- 0.47
CSF-based ptau^, Mean +/-SD	3.28+/- 0.50	2.74+/- 0.37
CSF-based αSyn^, Mean +/-SD	4.04+/- 0.07	1.91+/- 0.06†

Note: We did not compare statistically across variables due to the difference in data harmonization process.
^natural log transformed.
†log2 transformed during processing.
Abbreviations: αSyn, alpha-synuclein; Aβ, amyloid-beta; AD, Alzheimer's disease; ADNI, Alzheimer's Disease Neuroimaging Initiative; AQP4, Aquaporin-4; GFAP, glial fibrillary acidic protein; MCI, mild cognitive impairment; PD, Parkinson's disease; PPMI, Parkinson's Progression Markers Initiative; ptau, phosphorylated tau; YKL-40, chitinase-3-like protein 1.

αSyn were assayed using SomaLogic's SomaScan 7K (v4.1) platform at Washington University School of Medicine, St. Louis. The data are available in the 'CruchagaLab_CSF_metabolomic_matrix_20230620.csv' file in the ADNI database. CSF $A\beta_{1\text{-}42}$ and phosphorylated $ptau_{181}$ (ptau) were measured using Elecsys CSF immunoassays on a fully automated cobas e 601 analyzer (Roche Diagnostics) at the University of Pennsylvania. The data are available in the "UPENNBIOMK10.csv" file in the ADNI database. A natural log-transformation was applied to individual variables to normalize the data distribution.

PPMI

The lumbar puncture procedure in PPMI is described in the PPMI Biologics Manual (https://www.ppmi-info.org/sites/default/files/docs/PPMI%20Biologics%20Manual%20of%20Procedures%20V12.pdf). CSF GFAP, YKL40, AQP4, and αSyn were measured using the SOMAscan platform by Novartis Institutes for Biomedical Research (NIBR). The data are controlled for quality to remove outlier samples, calibrators, buffer, and non-human SOMAmers. The measured values are hybridization normalized, plate scaled, median normalized intra plate and calibrated at SomaLogic's side, then log2 transformed, median normalized inter plates at plate level. CSF $A\beta_{1\text{-}42}$ and $ptau_{181}$ were analyzed using the Elecsys $A\beta_{1\text{-}42}$, and $ptau_{181}$ electrochemiluminescence immunoassays on a fully automated cobas e 601 analyzer (Roche Diagnostics) by the Biomarker Research Laboratory, at the University of Pennsylvania. These immunoassays are currently under development and are for investigational use only. The $A\beta_{1\text{-}42}$ assay has a measurement range of 200 to 1700 pg/mL, and $ptau_{181}$ assay: 8 to 120 pg/mL. A natural log-transformation was applied to individual variables.

2.3.3 | DaTSCAN

PPMI

DaTSCAN ([123I]-FP-CIT SPECT) [(123) I-2β-carbomethoxy-3β-(4-iodophenyl)-N-(3-fluoropropyl) nortropane single photon emission computed tomography] imaging was acquired at PPMI imaging centers. Two hundred and forty out of 378 samples have clinician assessed dopamine transporter (DAT) status, and 237 out of 240 were positive cases at the screening timepoint. We conducted secondary analyses using only those with known DAT-positive status.

2.4 | Data analysis

2.4.1 | Characterization of astrocyte clusters

Pearson's correlation analysis was first used to examine correlations between individual astrocyte markers across ADNI and PPMI samples. The K-means clustering[37] was performed on the expression of the astrocyte markers GFAP, YKL40, and AQP4 from ADNI and PPMI samples (Figure 2A and E respectively). Clustering was conducted using a maximum of 10 iterations, requiring no change between iterations to achieve convergence. Visual inspection of the within-cluster sum of squared distances (WCSS, for compactness of clusters) as well as the silhouette coefficients (for separation of clusters) for candidate cluster solutions from 1 to 10 (Figure 2B and F) were used to determine the optimal number of clusters. We also used Likelihood Ratio Test (LRT) to statistically compare model fit between different cluster numbers.

2.4.2 | Generalized linear model analysis

Across ADNI and PPMI samples, we compared the ND pathologies (i.e., Aβ, ptau, and αSyn) as well as NPS (i.e., primarily on total score, and post-hoc analysis with individual subdomain scores) between astrocyte clusters using generalized linear models (GLMs). The model was structured as: $y = \beta 0 + \beta 1 Cluster + \epsilon$, where y referred to a pathology or NPS score, and a reference cluster was chosen to compare with the β1Cluster. For post-hoc analyses with NPS domain scores, false discovery rate (FDR) correction was conducted across all individual NPS domains. We conducted GLMs with and without age and ND diagnosis as covariates. When examining the interaction between astrocyte clusters and ND pathologies for NPS, we used a model structured as $y = \beta 0 + \beta 1 Cluster + \beta 2 Pathology + \beta 3 Cluster \times Pathology + \epsilon$, where y referred to the NPS score, and pathology referred to individual ND pathologies. Across analyses, necessary covariates, including age and clinical severity of an ND, were considered whenever appropriate.

We conducted all analyses for the two datasets separately since the CSF biomarkers were calculated differently with difficulties for

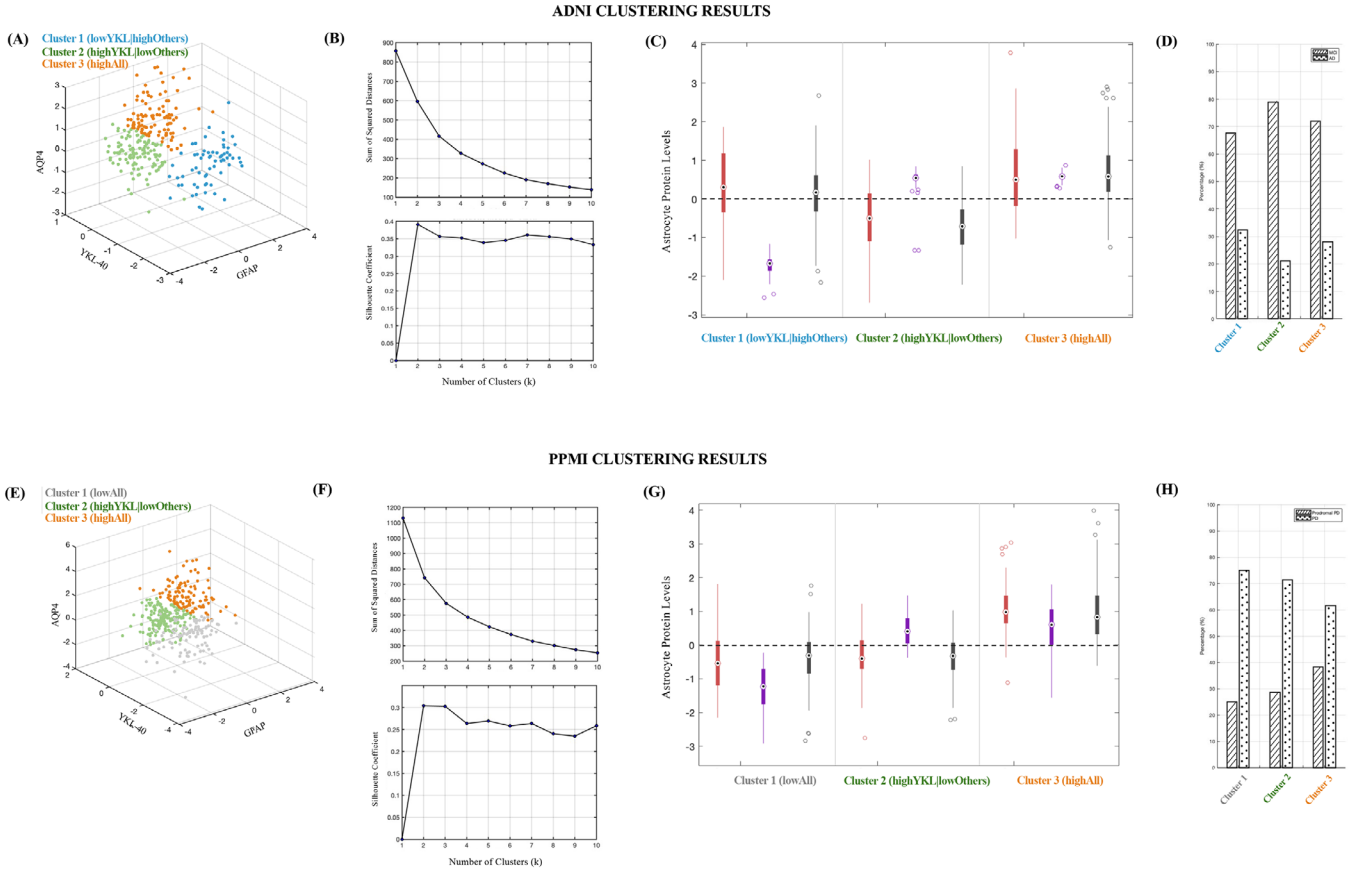

FIGURE 2 K-means clustering analysis for astrocyte biomarkers across ADNI and PPMI. The K-means clustering of distinct astrocyte biomarker patterns in (A) ADNI and (E) PPMI. Sum of squared distances across candidate cluster solutions in (B) ADNI and (F) PPMI. Astrocyte protein levels across clusters in (C) ADNI and (G) PPMI, in which red was for GFAP, purple for YKL-40, dark gray for AQP4. Distribution of preclinical and clinical ND in each cluster in (D) ADNI and (H) PPMI. ADNI, Alzheimer's Disease Neuroimaging Initiative; AQP4, aquaporin-4; GFAP, glial fibrillary acidic protein; ND, neurodegenerative disease; PPMI, Parkinson's Progression Markers Initiative; YKL-40, chitinase-3-like protein 1.

harmonization. We compare the similarities and differences across the two datasets in the Discussion section.

3 | RESULTS

3.1 | Cluster determination for astrocyte activity patterns in ADNI and PPMI samples

For ADNI sample, the optimal number of clusters K = 3 was identified via visual inspection of WCSS as well as consideration of silhouette coefficients for candidate cluster solutions from 1 to 10 (Figure 2B). These plots revealed a WCSS 'elbow' at K = 3 or K = 4 clusters, with a marginally higher silhouette coefficient when K = 3. LRT statistics suggested significant differences between K = 3 versus K = 2 (value = 404.15, $p < 0.001$) and K = 4 versus K = 3 (value = 35.66, $p < 0.001$). For PPMI sample, K = 3 was also identified via WCSS distances, silhouette coefficients for candidate cluster solutions from 1 to 10, and comparability with ADNI sample's cluster numbers (Figure 2F). LRT statistics suggested a significant difference between K = 3 versus K = 2 (value = 287.32, $p < 0.001$), but no difference between K = 3 versus K = 4 (value = 3.39, $p = 0.18$). Considering compactness, separation, and the need for cross-sample comparability, we selected K = 3 as the final clustering solution for both datasets.

3.2 | ADNI sample

3.2.1 | Astrocyte activity patterns

There was a significant positive correlation between levels of GFAP and AQP4 (r = 0.16, $p = 0.002$), but not between GFAP (r = -0.07, $p = 0.16$) or AQP4(r = -0.01, $p = 0.88$) and YKL-40.

The K-means clustering generated three clusters of distinct astrocyte activity patterns in the ADNI sample (Figure 2A). Cluster 1 (lowYKL|highOthers, $n = 68$) characterized by relatively low YKL-40 levels but high GFAP and AQP4 levels; Cluster 2 (highYKL|lowOthers, $n = 114$) characterized by relatively high YKL-40 levels but low GFAP and AQP4 levels; Cluster 3 (highAll, $n = 107$), characterized by consistently high values across all astrocyte markers, potentially reflecting the most severe astrocyte dysfunction (Figure 2C). Cluster 3, that is, "highAll," was used as the reference group in subsequent analyses

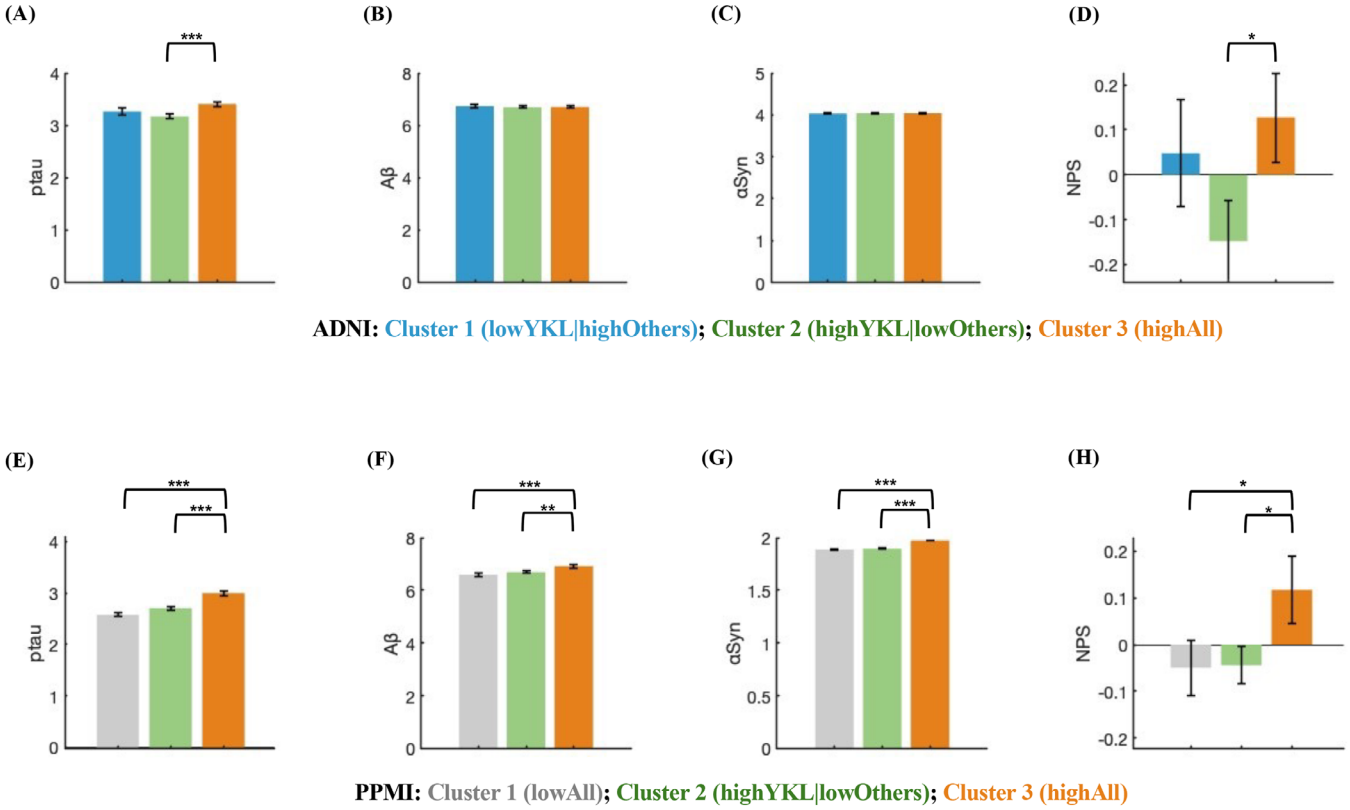

FIGURE 3 Comparisons of ND pathologies and NPS between astrocyte clusters in ADNI (A–D) and PPMI (E–H) with Cluster 3 considered as the reference. ADNI, Alzheimer's Disease Neuroimaging Initiative; Aβ, amyloid-beta; αSyn, alpha-synuclein; ND, neurodegenerative disease; NPS, neuropsychiatric symptoms; PPMI, Parkinson's Progression Markers Initiative; ptau, phosphorylated tau; $^{*}p < 0.05$;$^{**}p < 0.01$;$^{***}p < 0.001$.

when evaluating the relationships between astrocyte subtypes, ND pathologies, and NPS. There was no significant difference in clinical severity (MCI vs. AD dementia) between clusters ($\chi^2 = 3.07$, $p = 0.22$) (Figure 2D).

3.2.2 | Relationships between astrocyte clustering, ND pathologies, and NPS

Compared to the "highAll" cluster, there were significantly lower ptau levels in "highYKL|lowOthers" (B = -0.24, SE = 0.07, Wald's $\chi^2 = 12.62$, $p < 0.001$). Lower ptau levels were also observed in the "lowYKL|highOthers" cluster, though the difference was not significant (B = -0.32, SE = 0.08, Wald's $\chi^2 = 3.32$, $p = 0.069$) (Figure 3A). There was no by-cluster difference in Aβ or αSyn (Figure 3B and C).

Compared to the "highAll" cluster, there was significantly less severe NPS in "highYKL|lowOthers" (B = -0.33, SE = 0.13, Wald's $\chi^2 = 6.10$, $p = 0.014$), but no difference with the "lowYKL|highOthers" cluster (B = -0.16, SE = 0.16, Wald's $\chi^2 = 1.12$, $p = 0.29$), presented in Figure 3D. When controlling for AD/MCI diagnosis and age, results remained similar (Wald's $\chi^2 = 6.12$, $p = 0.013$).

When examining individual NPS domains (Figure 4A), after controlling for MCI/AD diagnoses and age, hallucinations (B = -0.29, SE = 0.14, Wald's $\chi^2 = 4.24$, $p = 0.039$), anxiety (B = -0.30, SE = 0.15, Wald's $\chi^2 = 3.94$, $p = 0.047$), disinhibition/compulsive behavior (B = -0.47, SE = 0.15, Wald's $\chi^2 = 10.19$, $p = 0.001$), and sleep and nighttime behaviors (B = -0.34, SE = 0.15, Wald's $\chi^2 = 5.39$, $p = 0.020$) were significantly different between "highYKL|lowOthers" and "highAll" clusters. Group difference in disinhibition/compulsive behavior remained significant after FDR correction (p = 0.010). Disinhibition/compulsive behavior (B = -0.50, SE = 0.17, Wald's $\chi^2 = 8.80$, $p = 0.003$) was significantly different between "lowYKL|highOthers" and "highAll" clusters but did not remain significantly different after FDR correction.

The difference in NPS severity between "highAll" and "highYKL|lowOthers" remained similar when controlling for Aβ, αSyn, or ptau individually (Wald's $\chi^2 = 5.21 - 6.26$, $p = 0.012$–0.022). Finally, we did not find any significant interaction between astrocyte clusters and individual ND pathologies for predicting NPS (Figure 5A-C).

3.3 | PPMI sample

3.3.1 | Astrocyte activity patterns

The three astrocyte activity measures were all correlated significantly (GFAP < > YKL-40: r = 0.35, $p < 0.001$; GFAP < > AQP4: r = 0.48, $p < 0.001$; YKL-40 < > AQP4: r = 0.18, $p < 0.001$).

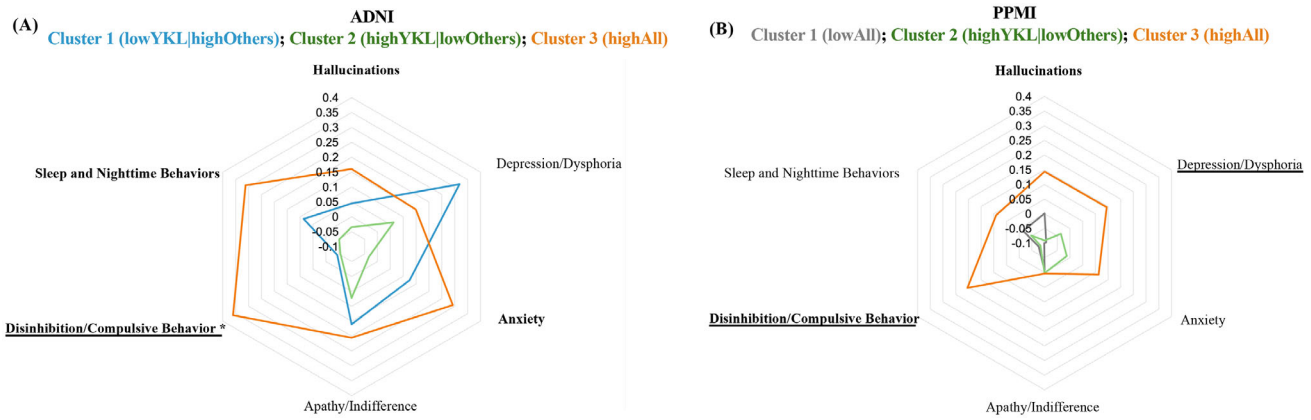

FIGURE 4 Comparison of NPS subdomains between astrocyte clusters in ADNI (A) and PPMI (B) with Cluster 3 considered as the reference. *Note*: Underline font: uncorrected significant difference between Cluster 1 and Cluster 3; **Bolden font**: uncorrected significant difference between Cluster 2 and Cluster 3; **Bolden underline font:** uncorrected significant difference between both Cluster 1 and Cluster 3, and Cluster 2 and Cluster 3. *FDR corrected significant difference. ADNI, Alzheimer's Disease Neuroimaging Initiative; FDR, false discovery rate; NPS, neuropsychiatric symptoms; PPMI, Parkinson's Progression Markers Initiative.

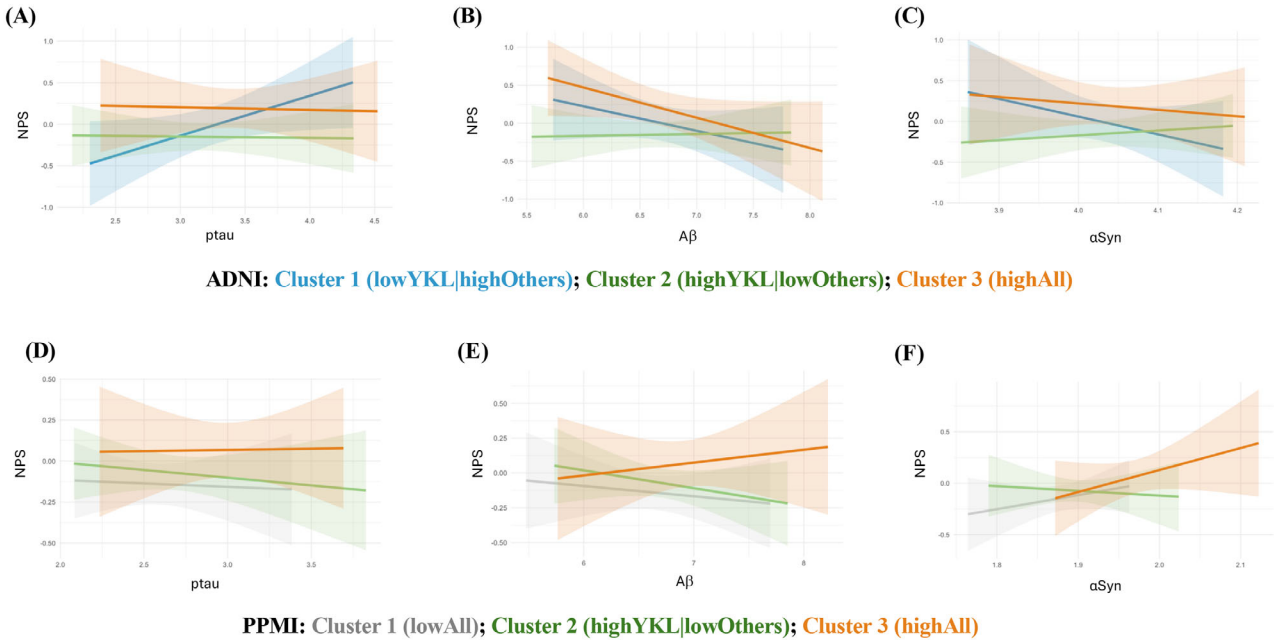

FIGURE 5 Relationship between ND Pathologies and NPS moderated by astrocyte clusters in ADNI (A–C) and PPMI (D–F) with Cluster 3 as the reference. *Note*: The shaded area represents the 95% confidence interval. There was a significant interaction between Cluster 2 and Cluster 3 for αSyn and NPS in PPMI (**F**). ADNI, Alzheimer's Disease Neuroimaging Initiative; Aβ, amyloid-beta; αSyn, alpha-synuclein; ND, neurodegenerative disease; NPS, neuropsychiatric symptoms; PPMI, Parkinson's Progression Markers Initiative; ptau, phosphorylated tau.

The K-means clustering in the PPMI sample generated three clusters of distinct astrocyte activity patterns, consistent with the ADNI sample (Figure 2E). Two clusters, Cluster 3 (highAll, $n = 107$), characterized by consistently high values across all astrocytic markers, and Cluster 2 (highYKL|lowOthers, $n = 171$), characterized by high YKL-40 levels but low GFAP and AQP4 levels, were similar to ADNI findings. Cluster 1 ($n = 100$) in the PPMI sample was characterized by low values across all astrocytic markers, "lowAll," which differed from Cluster 1 in ADNI (Figure 2G). There was no significant difference in clinical severity (prodromal PD and PD) between clusters ($\chi^2 = 4.79$, $p = 0.09$) (Figure 2H).

3.3.2 | Relationships between astrocyte clustering, ND pathologies, and NPS

Compared to the "highAll" cluster, there was significantly lower ptau levels in "highYKL|lowOthers" (B = -0.29, SE = 0.06, Wald's $\chi^2 = 26.33$,

$p < 0.001$) and "lowAll" clusters (B = -0.42, SE = 0.06, Wald's $\chi^2 = 47.10$, $p < 0.001$), lower Aβ levels in the "highYKL|lowOthers" (B = -0.24, SE = 0.08, Wald's $\chi^2 = 9.66$, $p = 0.002$) and "lowAll" clusters (B = -0.34, SE = 0.08, Wald's $\chi^2 = 17.42$, $p < 0.001$), and lower αSyn levels in the "highYKL|lowOthers" (B = -0.08, SE = 0.26, Wald's $\chi^2 = 169.23$, $p < 0.001$) and "lowAll" clusters (B = -0.08, SE = 0.30, Wald's $\chi^2 = 167.81$, $p < 0.001$). See Figure 3E-G for individual ND pathologies by astrocyte clusters.

Compared to the "highAll" cluster, there were significantly less severe NPS in the "highYKL|lowOthers" (B = -0.16, SE = 0.07, Wald's $\chi^2 = 4.71$, $p = 0.030$) and "lowAll" clusters (B = -0.17, SE = 0.08, Wald's $\chi^2 = 3.93$, $p = 0.047$) shown in Figure 3H. When controlling for prodromal PD/PD diagnosis and age, results remained similar (compared to the "highAll" cluster, "highYKL|lowOthers" at Wald's $\chi^2 = 6.23$, $p = 0.013$, "lowAll" at Wald's $\chi^2 = 5.52$, $p = 0.019$).

When examining individual NPS domains (Figure 4B), after controlling for prodromal PD/PD diagnoses and age, hallucinations (B = -0.24, SE = 0.12, Wald's $\chi^2 = 3.92$, $p = 0.048$) and disinhibition/compulsive behavior (B = -0.32, SE = 0.12, Wald's $\chi^2 = 6.59$, $p = 0.010$) were significantly different between "highYKL|lowOthers" and "highAll" clusters. Depression/dysphoria (B = -0.29, SE = 0.14, Wald's $\chi^2 = 4.31$, $p = 0.040$) and disinhibition/compulsive behavior (B = -0.31, SE = 0.14, Wald's $\chi^2 = 4.96$, $p = 0.03$) were significantly different between "lowAll" and "highAll" clusters. None of these domains remained significant after FDR correction.

When controlling for Aβ, αSyn, or ptau individually, significant NPS differences between clusters largely disappeared. We next examined interactions between astrocyte clusters and individual ND pathologies on predicting NPS. There was a significant interaction between astrocyte clusters and αSyn, that is, the positive association between αSyn and NPS seen in the "highAll" cluster was diminished in the "highYKL|lowOthers" cluster (B = -4.19, SE = 1.59, Wald's $\chi^2 = 6.99$, $p = 0.008$), but there was no difference in the association between the "highAll" and the "lowAll" clusters (Figure 5F). We did not find significant interactions with other types of ND pathologies (Figure 5D and E).

3.4 | Supplemental analyses for ADNI and/or PPMI sample

Across ADNI and PPMI samples, we conducted clustering analyses regressing out global cognition, measured by Montreal Cognitive Assessment (MoCA) to evaluate the influence of cognitive statuses on clustering, and results remained similar (Supplemental materials). For ADNI, we repeated the analysis using the traditional 12 subdomain based NPI score, and results remained similar (Supplemental materials). For the PPMI sample, we conducted all main analyses using only those with known DAT+ cases, and results remained similar (Supplemental materials).

4 | DISCUSSION

We partially confirmed our hypotheses. First, we identified two consistent clusters of astrocytic biomarkers across AD and PD cohorts (Figure 2C and F): the "highAll" cluster, where GFAP, YKL-40, and AQP4 expression are all elevated, and the "highYKL|lowOthers" cluster, characterized by high YKL-40 expression but low GFAP and AQP4 expression. Both cohorts also revealed a third cluster with notably low YKL-40 expression, though GFAP and AQP4 expression patterns in this cluster differed between PD and AD groups. Second, as hypothesized, similar associations were observed across cohorts between astrocyte clusters and both the severity of NPS and the extent of ptau expression, a generic marker of brain aging and neurodegeneration (Figure 3A, D, E, and H). However, contrary to our expectations, the relationship between astrocyte clusters and ND-specific primary pathologies differed. In PD patients, astrocyte clusters were significantly related to both AD and PD primary pathologies (Aβ and αSyn, Figure 3F and G), and the positive association between αSyn and NPS was attenuated in the "highYKL|lowOthers" cluster compared to the "highAll" cluster. In AD patients, however, no associations were observed between astrocyte clusters and either pathology (Figure 3B and C).

The study primarily highlights a robust relationship between NPS and specific patterns of astrocyte clusters across NDs. The similarities in the astrocytic clusters—"highAll" and "highYKL|lowOthers"—observed in both PD and AD cohorts, which corresponded to differences in NPS severity, suggest a potentially maladaptive astrocytic response when activity is universally elevated regardless of ND type or clinical severity. Notably, differences in NPS severity between the "highYKL|lowOthers" and "highAll" clusters across PD and AD, as well as between the "lowAll" and "highAll" clusters in PD, but not between the "lowYKL|highOthers" and "highAll" clusters in AD, collectively indicate that low levels of GFAP and AQP4, rather than low YKL-40, may play a more protective role in managing NPS (see collective discussion about this point below). Additionally, findings from individual NPS subdomains, such as hallucinations and disinhibition/compulsive behavior, show differences between the "highAll" and "highYKL|lowOthers" clusters in both AD and PD, though some results did not survive FDR correction (Figure 4). Despite differences in NPS assessment methods—ADNI relying on informant-reported NPI data and PPMI using informant, self, and clinician reports—the consistent relationships between astrocytic activity patterns and NPS, both as a composite and in individual symptoms, underscore the potential importance of astrocytic profiles in influencing NPS outcomes.

The study also highlights both consistencies and discrepancies in the relationships between astrocyte clusters, ND pathologies, and their interaction with NPS across AD and PD. Consistent differences in ptau levels were observed between the "highAll" and "highYKL|lowOthers" clusters in both AD and PD. However, differences in Aβ and αSyn levels were only evident between the "highAll" cluster and the other two clusters in PD, but not in AD. Furthermore, an interaction between

astrocyte clusters, particularly the "highAll" and "highYKL|lowOthers" clusters, and the effect of αSyn on NPS was observed in PD (Figure 5F) but not in AD. These findings suggest that, in PD, low GFAP and AQP4 levels may protect against the adverse effects of αSyn on NPS, consistent with the known bidirectional relationship between αSyn and glial cells in promoting neurodegeneration.[38,39] However, the reason for the association between astrocyte clusters and Aβ in PD, but not AD, remains unclear. While these astrocytic proteins have well-characterized roles in astrocyte function[40–44] and are studied in CSF for their connection to astrocyte reactivity and ND outcomes,[19–25,45,46] their expression may vary by brain region and is not specific to regions affected by AD or PD.[47,48] Further investigation using more sensitive astrocytic markers is warranted to better understand these relationships and overcome the limitations of current biomarkers.

Finally, we want to speculate on the distinct roles of AQP4, GFAP, and YKL-40 in astrocyte function. AQP4 and GFAP are thought to be critical to astrocyte-mediated homeostasis, with GFAP being linked to the maintenance of astrocytic structure and repair, and AQP4 related to the regulation of water transport across the blood–brain barrier (BBB).[40,44] Together, they are thought to support the astrocyte endfeet, which maintain BBB integrity and facilitate the clearance of toxic metabolites, including tau aggregates, through the glymphatic system.[42,43] In contrast, YKL-40 is considered a marker of astrocytic activation, often linked to neuroinflammation.[49] Our findings suggest that AQP4 and GFAP may be associated with synchronized homeostatic processes, while YKL-40 reflects a more generalized neuroinflammatory response. This could explain the greater NPS severity and tau accumulation in the "highAll" clusters of AD and PD patients, where high AQP4 and GFAP levels may indicate failed homeostatic processes exacerbated by neuroinflammation. Conversely, lower AQP4 and GFAP levels may preserve astrocytic homeostasis, potentially buffering against the effects of neuroinflammation and pathology, as seen in the "highYKL|lowOthers" cluster, where the correlation between αSyn and NPS in PD is attenuated.

There are limitations in this study. First, while these proteins have well-established links to astrocyte function, they remain indirect and non-specific markers; these results will benefit from confirmatory findings from future in vitro studies that can directly image astrocyte function in human cells[50] or in vivo non-human animal work that can similarly provide more direct measures of astrocyte function in models of PD and AD.[51] Direct comparisons between ADNI and PPMI cohorts were not possible due to differences in acquisition and processing methods for astrocytic and pathological biomarkers and NPS measures. Second, the cross-sectional design limits causal inferences regarding the relationships among astrocyte clusters, pathology, and NPS, or between specific astrocytic markers. There is also significant known heterogeneity even within specific disease categories, for example, due to pathology spread/progression, medication use, and comorbidities that are particularly prevalent in older adults at risk for dementia. The primary goal of this paper was to compare AD with PD and we had limited power to perform exploratory analyses to detect interactions between all of these factors; however, future studies designed to look specifically at these factors within certain disease stages of AD or PD may help uncover further complexity in astrocyte markers. Third, alternative analytical approaches, such as machine learning and deep learning, may better characterize the complicated nonlinear relationships among astrocytic markers and their associations with key features of NDs in relation to NPS. However, these methods typically require relatively large sample sizes to be most effective.

In conclusion, this study systematically examined the relationship between NPS and astrocyte markers across NDs. The lower pathological burden and NPS severity in the "highYKL|lowOthers" cluster compared to the "highAll" cluster, as well as the reduced impact of pathology on NPS in PD, highlight the significant role of astrocytic activity in NPS development. The clustering of astrocytic protein expression further suggests a functional interplay between AQP4 and GFAP, potentially supporting neuronal and synaptic health. These findings emphasize the importance of astrocytic activity in understanding NPS in NDs and highlight astrocytic processes as promising therapeutic targets.

ACKNOWLEDGMENTS

ADNI Data collection and sharing for this project were funded by the Alzheimer's Disease Neuroimaging Initiative (ADNI) (National Institutes of Health Grant U01 AG024904) and DOD ADNI (Department of Defense award number W81XWH-12-2-0012). ADNI is funded by the National Institute on Aging, the National Institute of Biomedical Imaging and Bioengineering, and through generous contributions from the following: AbbVie, Alzheimer's Association; Alzheimer's Drug Discovery Foundation; Araclon Biotech; BioClinica, Inc.; Biogen; Bristol-Myers Squibb Company; CereSpir, Inc.; Cogstate; Eisai Inc.; Elan Pharmaceuticals, Inc.; Eli Lilly and Company; Euroimmun; F. Hoffmann-La Roche Ltd and its affiliated company Genentech, Inc.; Fujirebio; GE Healthcare; IXICO Ltd.; Janssen Alzheimer Immunotherapy Research & Development, LLC.; Johnson & Johnson Pharmaceutical Research & Development LLC.; Lumosity; Lundbeck; Merck & Co., Inc.; Meso Scale Diagnostics, LLC.; NeuroRx Research; Neurotrack Technologies; Novartis Pharmaceuticals Corporation; Pfizer Inc.; Piramal Imaging; Servier; Takeda Pharmaceutical Company; and Transition Therapeutics. The Canadian Institutes of Health Research is providing funds to support ADNI clinical sites in Canada. Private sector contributions are facilitated by the Foundation for the National Institutes of Health (www.fnih.org). The grantee organization is the Northern California Institute for Research and Education, and the study is coordinated by the Alzheimer's Therapeutic Research Institute at the University of Southern California. ADNI data are disseminated by the Laboratory for Neuro Imaging at the University of Southern California.

PPMI Data used in the preparation of this article were obtained on 2024-07-23 from the Parkinson's Progression Markers Initiative (PPMI) database (www.ppmi-info.org/access-dataspecimens/download-data), RRID:SCR_006431. For up-to-date information on the study, visit www.ppmi-info.org. PPMI – a public-private partnership – is funded by the Michael J. Fox Foundation for Parkinson's Research and funding partners, including 4D Pharma,

Abbvie, AcureX, Allergan, Amathus Therapeutics, Aligning Science Across Parkinson's, AskBio, Avid Radiopharmaceuticals, BIAL, BioArctic, Biogen, Biohaven, BioLegend, BlueRock Therapeutics, Bristol-Myers Squibb, Calico Labs, Capsida Biotherapeutics, Celgene, Cerevel Therapeutics, Coave Therapeutics, DaCapo Brainscience, Denali, Edmond J. Safra Foundation, Eli Lilly, Gain Therapeutics, GE Healthcare, Genentech, GSK, Golub Capital, Handl Therapeutics, Insitro, Jazz Pharmaceuticals, Johnson & Johnson Innovative Medicine, Lundbeck, Merck, Meso Scale Discovery, Mission Therapeutics, Neurocrine Biosciences, Neuron23, Neuropore, Pfizer, Piramal, Prevail Therapeutics, Roche, Sanofi, Servier, Sun Pharma Advanced Research Company, Takeda, Teva, UCB, Vanqua Bio, Verily, Voyager Therapeutics, the Weston Family Foundation and Yumanity Therapeutic.

The manuscript preparation was supported by NIH U24 AG072701 to F.V.L. and NIH 1K01AG086665 to A.T.

CONFLICT OF INTEREST STATEMENT

The authors declare no conflicts of interest. Author disclosures are available in supporting information.

CONSENT STATEMENT

The ADNI and PPMI studies obtained informed consent from all participants. This study involved secondary data analysis without protected health information and did not require additional consent.

ORCID

Oceanna Yueran Li https://orcid.org/0009-0005-0298-4052
F. Vankee Lin https://orcid.org/0000-0003-1945-0362

REFERENCES

1. Erkkinen MG, Kim MO, Geschwind MD. Clinical Neurology and Epidemiology of the Major Neurodegenerative Diseases. *Cold Spring Harb Perspect Biol*. 2018;10(4):a033118.
2. Aarsland D, Marsh L, Schrag A. Neuropsychiatric symptoms in Parkinson's disease. *Mov Disord*. 2009;24:2175-2186.
3. Lanctot KL, Amatniek J, Ancoli-Israel S, et al. Neuropsychiatric signs and symptoms of Alzheimer's disease: new treatment paradigms. *Alzheimers Dement (N Y)*. 2017;3:440-449.
4. Borsini A, Giacobbe J, Mandal G, Boldrini M. Acute and long-term effects of adolescence stress exposure on rodent adult hippocampal neurogenesis, cognition, and behaviour. *Mol Psychiatry*. 2023;28:4124-4137.
5. Sofroniew MV. Astrocyte Reactivity: subtypes, States, and Functions in CNS Innate Immunity. *Trends Immunol*. 2020;41:758-770.
6. Nagai J, Yu X, Papouin T, et al. Behaviorally consequential astrocytic regulation of neural circuits. *Neuron*. 2021;109:576-596.
7. Poskanzer KE, Yuste R. Astrocytes regulate cortical state switching in vivo. *Proc Natl Acad Sci U S A*. 2016;113:E2675-84.
8. Yu X, Taylor AMW, Nagai J, et al. Reducing Astrocyte Calcium Signaling In Vivo Alters Striatal Microcircuits and Causes Repetitive Behavior. *Neuron*. 2018;99:1170-1187.e9.
9. Wahis J, Baudon A, Althammer F, et al. Astrocytes mediate the effect of oxytocin in the central amygdala on neuronal activity and affective states in rodents. *Nat Neurosci*. 2021;24:529-541.
10. Cui Y, Yang Y, Ni Z, et al. Astroglial Kir4.1 in the lateral habenula drives neuronal bursts in depression. *Nature*. 2018;554:323-327.
11. Escartin C, Galea E, Lakatos A, et al. Reactive astrocyte nomenclature, definitions, and future directions. *Nat Neurosci*. 2021;24:312-325.
12. O'Leary LA, Mechawar N. Implication of cerebral astrocytes in major depression: a review of fine neuroanatomical evidence in humans. *Glia*. 2021;69:2077-2099.
13. Ben Haim L, Escartin C. Astrocytes and neuropsychiatric symptoms in neurodegenerative diseases: exploring the missing links. *Curr Opin Neurobiol*. 2022;72:63-71.
14. Matias I, Morgado J, Gomes FCA. Astrocyte Heterogeneity: impact to Brain Aging and Disease. *Front Aging Neurosci*. 2019;11:59.
15. Holt MG. Astrocyte heterogeneity and interactions with local neural circuits. *Essays Biochem*. 2023;67:93-106.
16. Liddelow SA, Guttenplan KA, Clarke LE, et al. Neurotoxic reactive astrocytes are induced by activated microglia. *Nature*. 2017;541:481-487.
17. Zador Z, Stiver S, Wang V, Manley GT. Role of aquaporin-4 in cerebral edema and stroke. *Handb Exp Pharmacol*. 2009(190):159-170.
18. Matute-Blanch C, Montalban X, Comabella M. Multiple sclerosis, and other demyelinating and autoimmune inflammatory diseases of the central nervous system. *Handb Clin Neurol*. 2017;146:67-84.
19. Pelkmans W, Shekari M, Brugulat-Serrat A, et al. Astrocyte biomarkers GFAP and YKL-40 mediate early Alzheimer's disease progression. *Alzheimers Dement*. 2024;20:483-493.
20. Bellaver B, Povala G, Ferreira PCL, et al. Astrocyte reactivity influences amyloid-beta effects on tau pathology in preclinical Alzheimer's disease. *Nat Med*. 2023;29:1775-1781.
21. Vergallo A, Lista S, Lemercier P, et al. Association of plasma YKL-40 with brain amyloid-beta levels, memory performance, and sex in subjective memory complainers. *Neurobiol Aging*. 2020;96:22-32.
22. Pase MP, Himali JJ, Puerta R, et al. Association of Plasma YKL-40 With MRI, CSF, and Cognitive Markers of Brain Health and Dementia. *Neurology*. 2024;102:e208075.
23. Peng S, Liu J, Liang C, Yang L, Wang G. Aquaporin-4 in glymphatic system, and its implication for central nervous system disorders. *Neurobiol Dis*. 2023;179:106035.
24. Silva I, Silva J, Ferreira R, Trigo D. Glymphatic system, AQP4, and their implications in Alzheimer's disease. *Neurol Res Pract*. 2021;3:5.
25. Arighi A, Arcaro M, Fumagalli GG, et al. Aquaporin-4 cerebrospinal fluid levels are higher in neurodegenerative dementia: looking at glymphatic system dysregulation. *Alzheimers Res Ther*. 2022;14:135.
26. Oeckl P, Weydt P, Steinacker P, et al. Different neuroinflammatory profile in amyotrophic lateral sclerosis and frontotemporal dementia is linked to the clinical phase. *J Neurol Neurosurg Psychiatry*. 2019;90:4-10.
27. Holst CB, Brochner CB, Vitting-Seerup K, Mollgard K. Astrogliogenesis in human fetal brain: complex spatiotemporal immunoreactivity patterns of GFAP, S100, AQP4 and YKL-40. *J Anat*. 2019;235:590-615.
28. Verkhratsky A, Butt A, Li B, et al. Astrocytes in human central nervous system diseases: a frontier for new therapies. *Signal Transduct Target Ther*. 2023;8:396.
29. Habes M, Grothe MJ, Tunc B, McMillan C, Wolk DA, Davatzikos C. Disentangling Heterogeneity in Alzheimer's Disease and Related Dementias Using Data-Driven Methods. *Biol Psychiatry*. 2020;88:70-82.
30. Marek K, Chowdhury S, Siderowf A, et al. The Parkinson's progression markers initiative (PPMI)—establishing a PD biomarker cohort. *Ann Clin Transl Neurol*. 2018;5:1460-1477.
31. Cummings JL. The Neuropsychiatric Inventory: assessing psychopathology in dementia patients. *Neurology*. 1997;48:S10-6.
32. Gallagher DA, Goetz CG, Stebbins G, Lees AJ, Schrag A. Validation of the MDS-UPDRS Part I for nonmotor symptoms in Parkinson's disease. *Mov Disord*. 2012;27:79-83.
33. Goetz CG, Tilley BC, Shaftman SR, et al. Movement Disorder Society-sponsored revision of the Unified Parkinson's Disease Rating Scale

(MDS-UPDRS): scale presentation and clinimetric testing results. *Mov Disord*. 2008;23:2129-2170.
34. Gaudry E, Vagg P, Spielberger CD. Validation of the State-Trait Distinction in Anxiety Research. *Multivariate Behav Res*. 1975;10:331-341.
35. Yesavage JA, Brink TL, Rose TL, et al. Development and validation of a geriatric depression screening scale: a preliminary report. *J Psychiatr Res*. 1982;17:37-49.
36. Weintraub D, Hoops S, Shea JA, et al. Validation of the questionnaire for impulsive-compulsive disorders in Parkinson's disease. *Mov Disord*. 2009;24:1461-1467.
37. Hartigan JA, Wong MA. Algorithm AS 136: a k-means clustering algorithm. *Journal of the Royal Statistical Society Series C (Applied Statistics)*. 1979;28:100-108.
38. Wang R, Ren H, Kaznacheyeva E, Lu X, Wang G. Association of Glial Activation and α-Synuclein Pathology in Parkinson's Disease. *Neurosci Bull*. 2023;39:479-490.
39. Tu HY, Yuan BS, Hou XO, et al. α-synuclein suppresses microglial autophagy and promotes neurodegeneration in a mouse model of Parkinson's disease. *Aging Cell*. 2021;20:e13522.
40. Middeldorp J, Hol EM. GFAP in health and disease. *Prog Neurobiol*. 2011;93:421-443.
41. Liddelow SA, Barres BA. Reactive Astrocytes: production, Function, and Therapeutic Potential. *Immunity*. 2017;46:957-967.
42. Ishida K, Yamada K, Nishiyama R, et al. Glymphatic system clears extracellular tau and protects from tau aggregation and neurodegeneration. *J Exp Med*. 2022;219(3):e20211275.
43. Brenner M. Role of GFAP in CNS injuries. *Neurosci Lett*. 2014;565:7-13.
44. Papadopoulos MC, Verkman AS. Aquaporin water channels in the nervous system. *Nat Rev Neurosci*. 2013;14:265-277.
45. Querol-Vilaseca M, Colom-Cadena M, Pegueroles J, et al. YKL-40 (Chitinase 3-like I) is expressed in a subset of astrocytes in Alzheimer's disease and other tauopathies. *J Neuroinflammation*. 2017;14:118.
46. Ferrari-Souza JP, Ferreira PCL, Bellaver B, et al. Astrocyte biomarker signatures of amyloid-beta and tau pathologies in Alzheimer's disease. *Mol Psychiatry*. 2022;27:4781-4789.
47. Rodriguez JJ, Yeh CY, Terzieva S, Olabarria M, Kulijewicz-Nawrot M, Verkhratsky A. Complex and region-specific changes in astroglial markers in the aging brain. *Neurobiol Aging*. 2014;35:15-23.
48. Kimelberg HK. The problem of astrocyte identity. *Neurochem Int*. 2004;45:191-202.
49. Bonneh-Barkay D, Wang G, Starkey A, Hamilton RL, Wiley CA. In vivo CHI3L1 (YKL-40) expression in astrocytes in acute and chronic neurological diseases. *J Neuroinflammation*. 2010;7:34.
50. Pant P, Kaur G, Seth P. In Vitro Models of Astrocytes: an Overview. *The Biology of Glial Cells: Recent Advances*. 2022:719-734.
51. Spanos F, Liddelow SA. An Overview of Astrocyte Responses in Genetically Induced Alzheimer's Disease Mouse Models. *Cells*. 2020;9(11):2415.

SUPPORTING INFORMATION

Additional supporting information can be found online in the Supporting Information section at the end of this article.

How to cite this article: Li OY, Shin S, Zhou S, Turnbull A, Lin FV. Relationships between neuropsychiatric symptoms, subtypes of astrocyte activities, and brain pathologies in Alzheimer's disease and Parkinson's disease. *Alzheimer's Dement*. 2025;21:e70242. https://doi.org/10.1002/alz.70242